

Sintering Resistance of Pt@SiO₂ Core-Shell Catalyst

Seunghyun Kim,^[a] Siwon Lee,^[a] and WooChul Jung*^[a]

Although core-shell catalysts have been actively studied for their excellent stability at high temperatures, most studies have focused on the development of synthetic methods and not conducted actual catalytic reactions at conditions, under which particles severely agglomerate. Here, we prepare a model catalyst with a well-defined size and interface of a Pt core and a gas-permeable SiO₂ shell *via* advanced colloidal synthesis, and evaluate the catalytic response to CO and CH₄ oxidation, each

representing low (<300 °C) and high (>500 °C) temperature reactions. Compared to typical SiO₂ supported Pt, the core-shell configuration shows comparable activity at CO oxidation and a much higher activity and stability for CH₄ oxidation. However, even for the core-shell, degradation is inevitable, and possible reasons for this are discussed. These practical results on high-temperature catalysis provide important evaluation criteria and design guidelines for sintering-resistant nanocatalysts.

Introduction

Silica-supported Pt nanoparticles are widely used in heterogeneous catalysis due to the high catalytic activity of Pt, the broad availability and stability of SiO₂, and the increasing dispersion of nanoscale particles.^[1] Therefore, it is of great academic and technical importance to establish guidelines for ideal catalyst designs for this system. A prerequisite for this would be research on the synthesis of silica-supported Pt nanocatalysts (Pt/SiO₂) of uniform size and distribution accompanied by a quantitative analysis of their reactivity and durability under reacting conditions. Meanwhile, the most important issue with regard to their catalytic application is the inherent thermal instability of Pt nanoparticles. Nano-sized particles are vulnerable to high temperatures and tend to agglomerate through the mechanisms of coalescence and/or Ostwald ripening^[2] to minimize their surface energy. Additionally, particle growth at high temperatures leads to a severe loss of the catalytically active surface area and performance degradation of the catalyst. This phenomenon cannot be overlooked given that many industrial applications of platinum nanocatalysts, such as automobile exhaust control and hydrocarbon reforming processes, are conducted in atmospheres with elevated temperatures (>500 °C).

In this regard, many studies are ongoing as part of the effort to address the thermal stability issue. The following are some of the suggested solutions that have received the most attention recently: alloying a Pt nanoparticle with other metals to obtain a higher melting temperature,^[3] adjusting an oxide support to obtain stronger anchorage with a metal,^[4] and forming a composite structure such as a core-shell configuration which physically protects Pt particles. Unlike the other solutions, the

core-shell structure can indisputably isolate each metal nanoparticle with the stable oxide shells to prevent migration and aggregation effectively, without restricting the catalyst chemical composition and thus the function.^[5] Moreover, by constructing shells with gas-permeable mesopores, this approach ensures sufficient catalytic activity. Accordingly, in many studies, the application of the core-shell configuration has shown great promise as a stable heterogeneous catalyst composed of Pt and SiO₂.^[6] For example, Kishida et al. prepared a silica-coated Pt metal nanocatalyst (Pt@SiO₂) through a microemulsion method, and it demonstrated superior selectivity for competitive hydrocarbon oxidation.^[6a] Another catalyst with Pt nanoparticles embedded in silica nanospheres was also synthesized and showed high performance for hydrogen generation.^[6b] Recently, the simple synthesis of a highly stable and active catalyst was proposed by Somorjai et al.^[6c] They designed their Pt@SiO₂ catalyst by synthesizing colloidal Pt cores and encaging them with a mesoporous silica shell. This model catalytic system maintained its structural endurance even after calcination at temperatures as high as 750 °C and presented decent catalytic activity toward CO oxidation and ethylene hydrogenation.

However, although the preceding studies suggest that the core-shell structure improves the sintering resistance of a Pt@SiO₂ catalyst, they mainly focused on the development of a synthetic method itself, whereas few studies have systematically investigated whether the catalyst is suitable for practical applications. Indeed, for this type of catalyst, previous studies lack catalytic reactions at elevated temperatures (>500 °C) and long-term stability tests under practical atmospheres. Therefore, it is essential to synthesize Pt@SiO₂ particles uniformly controlled in terms of the size and distribution and to evaluate their reactivity and durability at high temperatures.

In this work, we test the feasibility of the high-temperature catalysis of Pt@SiO₂ nanoparticles. First, we prepare Pt particles with a narrow size distribution using cationic surfactants, wrap them with silica precursors, and obtain core-shell particles through a subsequent heat treatment. For comparison, Pt/SiO₂ with the same Pt size are also prepared as a conventional reference catalyst. Transmission electron microscopy (TEM), X-ray diffractometer (XRD), and CO chemisorption analyses reveal

[a] S. Kim, S. Lee, Prof. W. Jung
Department of Materials Science and Engineering
Korea Advanced Institute of Science and Technology (KAIST)
291 Daehak-ro, Yuseong-gu
Daejeon 34141 (Republic of Korea)
E-mail: wcjung@kaist.ac.kr

Supporting information for this article is available on the WWW under <https://doi.org/10.1002/cctc.201900934>

that the synthesized Pt@SiO₂ is highly monodisperse, gas permeable, and apparently stable up to 650 °C. The core-shell catalysts show reactivity comparable with the reference catalysts under relatively low-temperature (<300 °C) reactions such as CO oxidation, despite the fact that their surfaces are partially covered with silica. On the other hand, when used for methane oxidation at much higher temperatures (>500 °C), the core-shell configuration substantially decelerates the degradation of the catalyst, thus proving itself as a suitable candidate for high-temperature heterogeneous catalysis. However, we observe that, unlike expectations, catalytic activity degradation arises to some extent. The results presented above clearly demonstrate the advantages and disadvantages of the core-shell catalyst and suggest that controlling the structure and durability of the inorganic shell is key with regard to the development of high-performance catalysts with long lifetimes.

Results and Discussion

Pt@SiO₂ core-shell catalysts were prepared in four steps: (1) the colloidal synthesis of Pt particles, (2) silica shell formation by hydrolysis and condensation of Si precursors, (3) the adsorption of as-synthesized Pt@SiO₂ core-shell composites on an additional silica support, and (4) calcination. First, monodisperse Pt particles were obtained by aqueous-based colloidal synthesis using C₁₆TABr, a cationic surfactant. This method of using an ionic surfactant is not only simple and easy, but it is also very effective in controlling the shape and size of the particles, while maintaining high dispersion.^[7] In this case, K₂PtCl₄, a precursor, was mixed with C₁₆TABr to form a Pt complex. Subsequently, the mixture solution was reduced with NaBH₄ to synthesize Pt nanoparticles with a narrow particle distribution. A procedure of covering each Pt core with silica shells followed to protect individual cores under high temperatures.^[6c] When Si precursor, tetraethyl orthosilicate (TEOS), and pre-synthesized Pt nanoparticles were mixed in a basic aqueous solution; the basicity of the solution causes the hydrolysis and condensation of TEOS and eventually converts it to SiO₂. During this process, the cationic surfactant not only helps to disperse nano-sized Pt particles but also serves as a structural templating agent for silica formation. Therefore, polymerization takes place around the Pt core forming an as-synthesized Pt@SiO₂ core-shell composite. As-prepared Pt@SiO₂ composites were then supported on additional silica nanopowders for characterization and catalysis.

Despite the wide use of the encapsulating method in many studies,^[8] there is very limited discussions about its synthetic details.^[9] Here are some noteworthy aspects to be considered during the optimization of the catalyst structure. In order to prevent each Pt core from aggregating, it is important to isolate one Pt particle in a single shell. It would be of no use if one shell contains several cores, as they can easily agglomerate and grow into larger particles inside the shell when encountering a high-temperature condition. By controlling the amount of surfactants attached to each Pt nanoparticle, separation of the cores could be achieved. After Pt nanoparticle synthesis, harsh

centrifuging resulted in insufficient surfactant around the Pt cores, leading to poor dispersion of the particles and thus the formation of several cores in a shell, as displayed in Figure S1. Likewise, the thickness of a silica shell could be altered by controlling the amount of TEOS added during the synthesis step. When more TEOS was added, thicker silica shells could be formed as shown in Figure S2. Because a thin silica shell leads to an unstable catalyst that cannot maintain its structure or core size at a high temperature^[5a] (Figure S3), we controlled the thickness of the silica shell by ensuring that it is thick enough (28.5 ± 1.7 nm) to withstand calcination at 650 °C. Additionally, to effectively distribute core-shell particles for use as a catalyst, electrostatic interaction between positively charged as-synthesized Pt@SiO₂ composites and negatively charged silica nanopowders in a basic solution^[10] was used. When they were mixed, the sediment powders were formed immediately and through calcination, surfactants were eliminated and mesopores were created.

The morphologies of the as-synthesized Pt particles and Pt@SiO₂ composites are shown in Figure 1. Pt nanoparticles displayed a narrow size distribution with a diameter of 9.7 ± 0.8 nm, and each Pt core is encaged uniformly in a silica shell. The energy dispersive spectroscopy (EDS) mapping and line scan in Figure 1 (c, d) confirms the composition of the Pt core in the middle and the SiO₂ shell surrounding it. In Figure 1 (b), excess silica particles are also observable; however, no extra procedure to remove these residuals is necessary because, as explained earlier, the as-synthesized Pt@SiO₂ composites are supported on additional silica nanopowders for actual catalyst measurements anyways. The conventional supported type Pt/SiO₂ shown in Figure S4 was fabricated through dispersion of Pt nanoparticles, synthesized with the same method. The uniform Pt size distribution is confirmed, which makes the sample suitable for a reasonable comparison with the core-shell catalyst. The final Pt@SiO₂ catalyst was targeted to contain 0.7 wt.% Pt calculated based on the inductively coupled plasma optical emission spectrometer (ICP-OES) measurement of the colloidal Pt nanoparticle solution (Table S1). The same amount of Pt was included in the reference Pt/SiO₂ catalyst for comparison. After calcination, the silica shell becomes highly mesoporous, as confirmed through a CO chemisorption measurement. The CO adsorption behavior of the sample indicates that there is 0.127 m²/g_{cat} of exposed metallic surface area due to the numerous mesopores in the silica shell. Assuming that all the Pt nanoparticles have sphere shapes with 9.7 nm in diameter and that the entire surface area can be utilized without any blockage from the oxide support, the exposed metallic surface area of the catalyst is calculated to be 0.202 m²/g_{cat}. This indicates that once the surfactants are removed by thermal decomposition, the space previously occupied by them become highly gas-permeable channels,^[5a,6c] thus allowing more than a half of the ideal Pt surface to be exposed to reactant gas. Nitrogen physisorption results re-confirmed that the core-shell structures contain an abundance of 2~3 nm sized pores and has a specific surface area of 451.0 m²/g_{cat}. This porous structure and the resulting gas permeability of the catalyst show that it can be utilized as a heterogeneous catalyst.

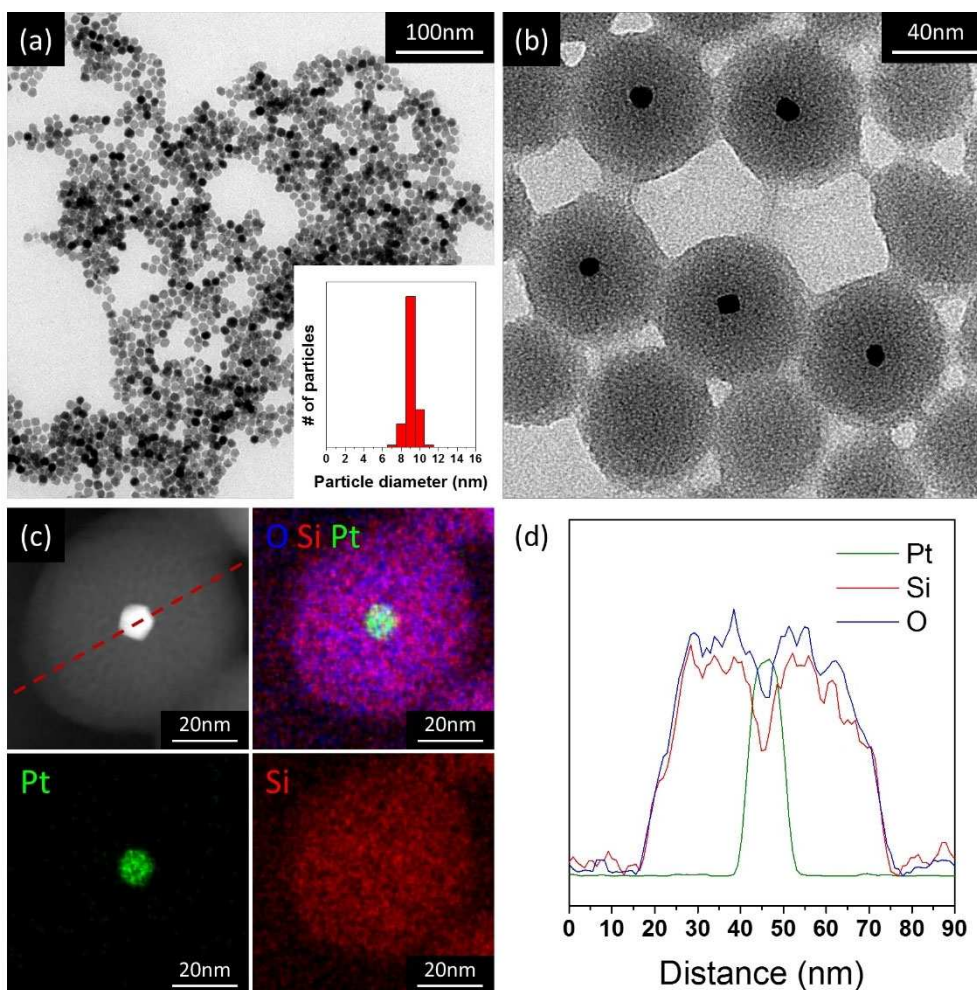


Figure 1. TEM image of as-synthesized Pt nanoparticles (a); the inserted graph is the particle size distribution. TEM image (b), TEM-EDS mapping (c), and TEM-EDS line scan (d) of as-synthesized Pt@SiO₂ composite.

Additionally, the XRD pattern in Figure 2 (b) reveals that the core-shell catalyst consists of crystalline Pt and amorphous silica even after calcination.

To investigate the sintering resistance of the core-shell particles, they were placed in a thermally harsh condition of 650 °C, which is higher than the operating temperature of the target reaction, CH₄ oxidation. According to TEM images, the

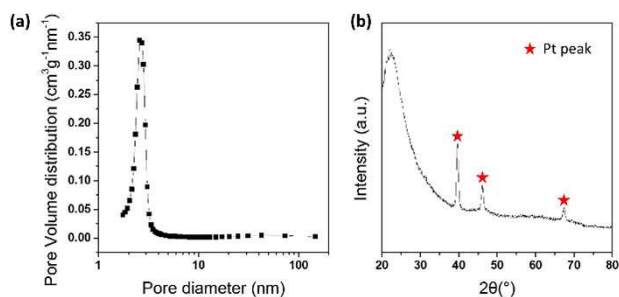


Figure 2. Pore size distribution calculated from the N₂ adsorption isotherm (a), and XRD data (b) of the Pt@SiO₂ catalyst.

conventional supported type of catalyst showed severe agglomeration after merely three hours of annealing, whereas the core-shell catalyst remained its core-shell structure and the particles rarely aggregated, as can be observed in Figure 3. For some Pt nanoparticles in Pt/SiO₂, the diameters grew to as much as five times their original size. Assuming that the particles all have spherical shapes, this degree of particle growth causes a decrease in the metallic surface area to 1/22 of the original. According to these morphological analysis results, catalytic activity degradation at a high temperature is likely to be inevitable for the Pt/SiO₂ catalyst due to the decrease in the catalytically active metallic surface area followed by the increase in the Pt nanoparticle size.

The catalytic properties of the Pt@SiO₂ catalyst at moderate temperatures have been assessed through CO oxidation tests. In the present study, we measured the reaction rate of the Pt@SiO₂ catalyst in the temperature range of 100~300 °C, and the Pt/SiO₂ catalyst as well, as a comparison. The maximum temperature used, 300 °C, is lower than the pre-annealing temperatures of the catalysts, implying that both catalysts are thermally stable during the reaction. Through the fact that the

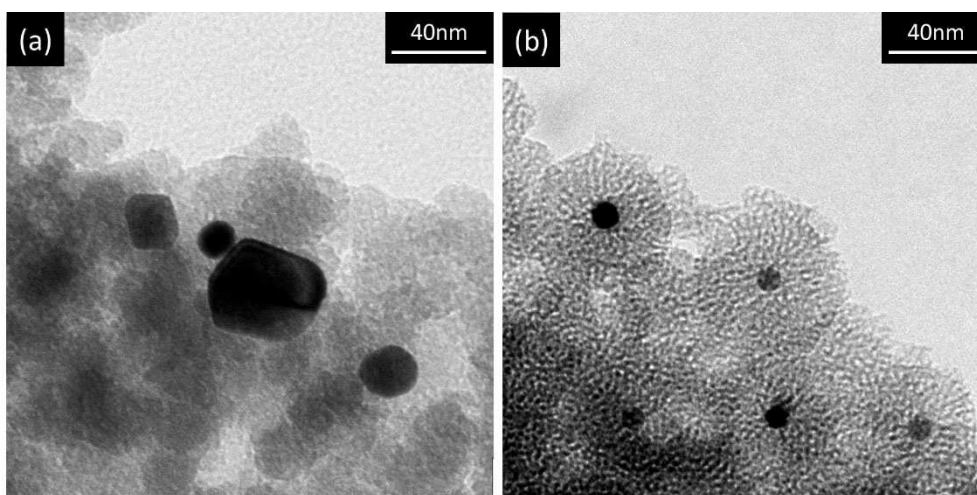


Figure 3. TEM images of Pt/SiO₂ (a), and Pt@SiO₂ (b) after a thermal treatment at 650 °C for three hours in air.

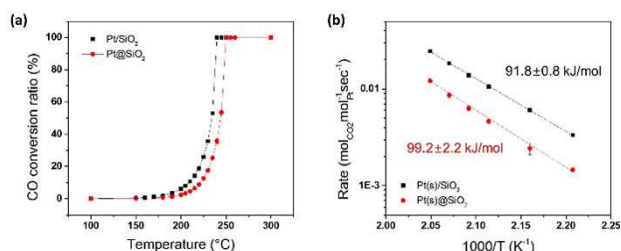


Figure 4. Light-off curve of CO conversion with respect to the temperature (a), and kinetic data (b) for Pt/SiO₂ and the Pt@SiO₂ catalyst.

core-shell catalyst shows decent catalytic activity, as presented in Figure 4, the gas accessibility of the silica shell is reconfirmed. Figure 4 (a) shows the conversion ratio of CO for each catalyst with respect to the temperature. Throughout the entire temperature range, the supported-type catalyst exhibited a comparable but slightly higher conversion ratio than the core-shell-type catalyst. The catalytically inert nature of silica makes the Pt surface the only active site for the oxidation reaction.^[11] Therefore, the small difference in the catalytic activity may be due to the difference in the exposed metallic surface area caused by the presence of the silica shell on the Pt nanoparticle surface. Figure 4 (b) presents the kinetic rate data of the reaction. To analyze the intrinsic properties of the catalysts without thermal effects, temperature ranges with a 2~10% CO conversion ratio were selected. Both the core-shell and the supported-type catalyst showed similar apparent activation energy of 99.2 ± 2.2 kJ/mol and 91.8 ± 0.8 kJ/mol, respectively. Accordingly, although there is a slight difference in the magnitude of the activity, the reaction mechanism is considered to be identical for both catalysts.

For high-temperature CH₄ oxidation, which maximizes the advantage of core-shell structures, the reacting temperature was increased to 570 °C, a temperature high enough for a conventionally synthesized supported type of catalyst to be sintered and degraded. Inevitably, the Pt/SiO₂ catalyst suffered

degradation simultaneously as the temperature was increased, in turn exhibiting slower CH₄ conversion than Pt@SiO₂ at all temperatures higher than 400 °C,^[12] as shown in Figure 5 (a). For practical use of the catalyst, it must maintain stable activity throughout the reaction, which would take place at a high temperature for a long time. Therefore, long-term CH₄ oxidation was tested at 560 °C and the turnover frequency value was calculated to determine the catalytic activity evolution over time. Because sintering and degradation had occurred as the temperature had been increased, the Pt/SiO₂ catalyst showed a much lower turnover frequency value from the beginning of the long-term measurement. As time elapsed, more aggregation took place, and in only 20 hours, the turnover frequency dropped dramatically to only 40% of the starting value and the CH₄ conversion ratio dropped to less than 10%. The reason for the activity degradation can be seen in the TEM image in Figure 5 (c) as the particle size distribution shifted significantly to larger particles. In the case of the core-shell type Pt@SiO₂ catalyst, it showed much higher CH₄ conversion due to sintering resistance coming from the physical protection of the silica shell. Particularly at the beginning of the reaction (<20 hours), the differences are more extreme. It is clear that the shells have succeeded in slowing down the degradation process. However, they could not stop the degradation completely. The turnover frequency of Pt@SiO₂ decreased slowly to 60% after 100 hours, matching the decrease in conversion ratio of methane.

We suggest three possible reasons for the degradation of the core-shell catalyst. First, the silica shell may not have been a perfect protection of the Pt cores and thus may have allowed Pt particles to diffuse through the mesopores and aggregate *via* the mechanism of Ostwald ripening. In this case, some Pt nanoparticles with diameters even smaller than the original size (9.7 nm) are expected to be discovered after high-temperature measurements. Second, even with the optimization procedure to synthesize a uniform catalyst that contains one Pt core each, little portion of the core-shell structure may have had more than one Pt nanoparticle from the beginning. This would cause

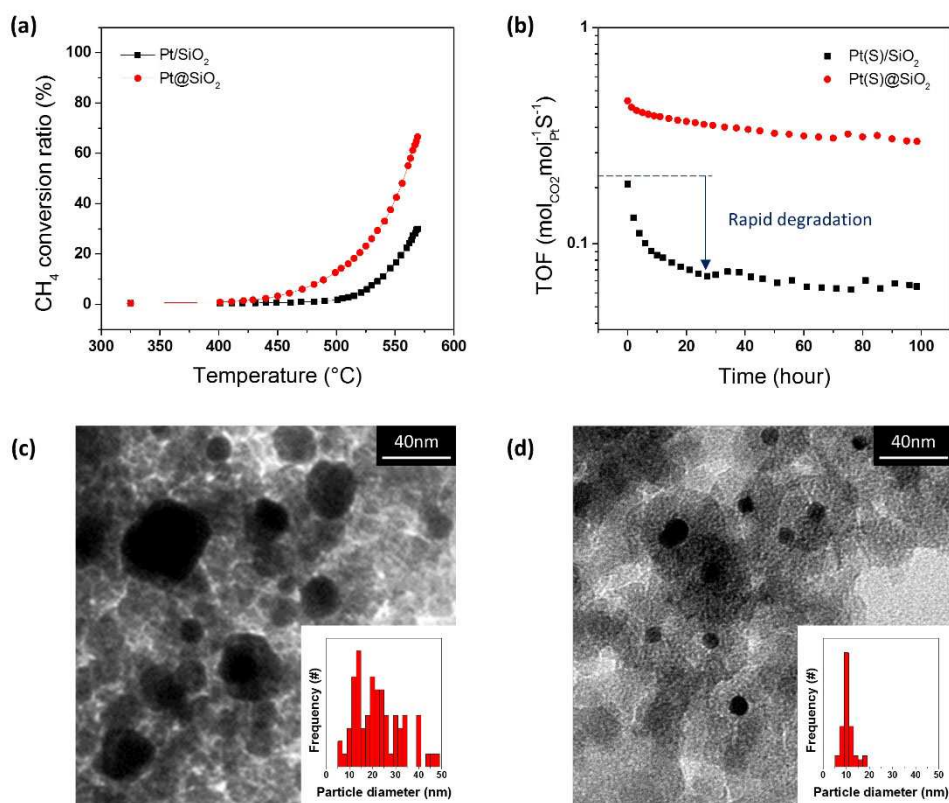


Figure 5. Light-off curve of CH₄ conversion with respect to the temperature (a), and turn over frequency change in CH₄ oxidation in terms of time (b) for Pt/SiO₂ and Pt@SiO₂ catalyst. TEM images of Pt@SiO₂ (c) and Pt/SiO₂ (d) after long-term CH₄ oxidation measurements for 100 hours at 560 °C; the inserted graph shows the particle size distributions for Pt@SiO₂ (c) and Pt/SiO₂ (d) after long-term CH₄ oxidation measurements.

cores to agglomerate inside the shell and grow into a larger size. In fact, changes in the size distribution of the Pt particles before and after the high-temperature reactions through the TEM image analysis shown in Figure 5 (d) indicates that these two phenomena actually took place. Both shrunken and enlarged nanoparticles compared to those before the reaction can be found. Based on these observations, we propose to improve the dispersity of Pt particles and to increase the shell thickness to suppress the diffusion of Pt atoms in order to improve the core-shell catalyst performance further. Next, we can conceive of one additional reason for the thermal degradation of the catalyst that does not accompany growth of the Pt size. The morphology of the silica shell itself might have been deformed and may have then blocked the mesopores, thus prohibiting access of the reactant gas. In fact, by calculating the average nanoparticle size growth observed from the TEM images, we can predict that the total exposed metallic surface area decreased to ~90% of the original. However, the reaction rate decreased on a larger scale, which is the outcome of the additional degradation from the shells that cannot be observed in the TEM image. Hence, to solve this problem, shells with greater thermal stability should be used. It would be better if the shell could improve catalytic activity *via* strong metal-support interaction with Pt cores. Overall, these observations from the long-term test imply that examining the catalytic activity under actual high-temperature reacting conditions for a

sufficient amount of time is very important for confirming the feasibility of the synthesized catalysts. The perfectly stable morphology after a short thermal treatment did not correspond to the thermal stability of the catalyst, and even the core-shell configuration could not bear the harsh reacting condition for the long times used here. However, it still showed a much higher conversion rate than the conventional supported type of catalyst and demonstrated strong potential for use in actual applications. Nonetheless, a careful examination is necessary for further development of this catalyst.

Conclusions

In conclusion, a core-shell catalyst consisting of a Pt nanoparticle and a mesoporous silica shell was successfully synthesized as a high-temperature oxidation catalyst. A washing procedure of the as-synthesized Pt nanoparticles affected the amount of surfactants attached to the Pt cores, which was important for each silica shell to contain a single Pt core. It was also found that the silica shell thickness could be modified by the amount of TEOS added during the polymerization process and that a certain thickness was required for the shell to protect the nano-sized Pt particles effectively from sintering at high temperatures.

This nanocomposite has been tested as a catalyst for CO oxidation, and it showed activation energy similar to that of a conventional supported-type catalyst, indicating an identical oxidation reaction mechanism. Pt@SiO₂ also showed decent catalytic activity, which was only slightly lower than that of the Pt/SiO₂ catalyst due to the slightly smaller exposed metallic surface area. To test its role as a catalyst for high-temperature reactions, CH₄ oxidation tests were conducted. The effective protection of the silica shell was noted through the superior catalysis compared to an agglomerated Pt/SiO₂ catalyst.

Despite the outstanding catalytic activity of Pt@SiO₂ during high-temperature methane oxidation, it could not last long. Even in the core-shell catalyst, degradation occurred. This phenomenon appears to be caused by the combination of aggregation of the Pt nanoparticles and deformation of the silica shell. This observation suggests future directions for improving the stability of core-shell catalysts and expands the guidelines for ideal characterization during the development of sintering-resistant catalysts that can be applied to practical high-temperature reactions. Clearly, the apparently stable images of particles after short calcination are not sufficient, and actual measurements of the catalytic activity under practical conditions for a long time are crucial. Meanwhile, this study nonetheless demonstrated the possibility of a core-shell structure for slowing the agglomeration of Pt nanoparticles, and such a structure can also be utilized in more fundamental studies that do not involve long-term exposure at an elevated temperature. We also suggest that careful selection of robust shell materials and an optimized synthetic method for more uniform catalysts would be necessary for further development of sintering-resistant core-shell catalysts.

Experimental Section

Preparation of Pt Nanoparticles

Pt nanoparticles, stabilized with cationic surfactant, were prepared through colloidal synthesis.^[13] 1.822 g of hexadecyltrimethylammonium bromide (C₁₆TABr), the surfactant, was mixed with 42 mL of deionized water in a round bottom flask, and aqueous solution of potassium tetrachloroplatinate (K₂PtCl₄), a precursor, (10 mM, 5 mL) was added to the mixture. The flask was sealed with rubber septum, and the mixture was stirred at 300 rpm for 10 min. Subsequently, the flask containing the mixture was heated to 50 °C in silicon oil bath until the surfactants dissolved, and the solution became nearly transparent. Ice-cooled aqueous solution of sodium borohydride (NaBH₄, 500 mM, 3 mL) was then added with a syringe. Through a needle of the syringe, H₂ gas generated inside the flask was released for 20 min. The solution was maintained stirring at 300 rpm at 50 °C for 15 hours, and eventually the solution turned brown. Pt nanoparticles were then collected from the solutions through appropriate centrifuging and were re-dispersed in 5 mL of deionized water for further use.

Preparation of as-Synthesized Pt@SiO₂ Composites

40 mL aqueous solution of 10 mM tetradecyltrimethylammonium bromide (C₁₄TABr) was prepared with 0.1 mL of ammonia added to adjust the pH of the solution to be 10~11. To this solution, 0.5 mL

of the colloidal Pt nanoparticle solution was added with stirring (500 rpm). After 10 minutes for the Pt nanoparticles to be stabilized and dispersed, 3 mL of 10 vol.% TEOS diluted with ethanol, was added for silica formation. The mixture was stirred (500 rpm) for 1 hour as encapsulation of Pt nanoparticles with silica shells took place. The resulting solution was then centrifuged at 12000 rpm for 15 minutes and was re-dispersed in deionized water for TEM analysis.

Preparation of Silica-Supported Pt@SiO₂ Catalyst

200 mg of silica nanopowder, dispersed in 200 mL of deionized water modified to be basic (pH = ~10) by adding ammonia, has a negative surface charge. To this mixture, appropriate amount of as-synthesized Pt@SiO₂ composites (to achieve final loading of 0.7 wt.% Pt), which have positive charge due to cationic surfactants, was added with stirring (500 rpm) for 30 min. Electrostatic interaction adsorbed the as-synthesized Pt@SiO₂ composites onto the silica nanopowder support and Pt@SiO₂/SiO₂ appeared as a sediment. After removing the supernatant liquid, it was dried at 80 °C overnight and was calcined at 450 °C for 3 hours. Calcination process removed the remaining surfactants and TEOS residues thus creating mesopores in the silica shell and creating Pt@SiO₂ catalyst.

Preparation of Pt/SiO₂ Catalyst

200 mg of silica nanopowder was mixed with an appropriate amount of Pt nanoparticle solution (to achieve final loading of 0.7 wt.% Pt) with stirring (500 rpm) for 10 min. Adsorption of Pt nanoparticles on the silica nanopowder support occurred. The solution was dried at 80 °C overnight, and was calcined at 350 °C for 5 hours to remove the remaining surfactants.

Characterization Techniques

For TEM analysis of the Pt nanoparticles, as-synthesized Pt@SiO₂ composites, Pt@SiO₂ catalyst and Pt/SiO₂ catalyst, JEOL JEM-3010 operated at 300 kV and Talos F200X operated at 200 kV was used. ICP-OES (Agilent ICP-OES 7700 S) confirmed the concentration of Pt for each catalyst sample. The crystal structure of the sample was identified with XRD using a RIGAKU D/MAX-2500 with Cu-K α irradiation at 40 kV and 200 mA. CO chemisorption was carried out at 35 °C using ASAP 2020 C, to estimate the metallic surface area of the catalyst sample. Micromeritics 3 flex was used to measure N₂ adsorption-desorption isotherm, so pore distribution and Brunauer-Emmett-Teller (BET) specific surface area of the core-shell catalyst could be obtained.

Catalytic Test

CO oxidation and CH₄ oxidation were conducted in a fixed-bed flow quartz reactor. In the catalytic bed, 50 mg of catalyst mixed with 200 mg quartz sand was placed in between 100 mg quartz sand layer, and quartz wool layer was in the bottom supporting the system. K-type thermocouple was placed right below and next to the catalytic bed to measure the temperature. For CO oxidation, 1 vol.% CO, 4 vol.% O₂, and 95 vol.% Ar was flowed at 50 mL/min with gas hourly space velocity (GHSV) corresponding to 60000 mL·g⁻¹·h⁻¹. For the long-term CH₄ oxidation, harsher condition of 1.33 vol.% CH₄, 6.67 vol.% O₂, and 92 vol.% Ar was fed at 150 mL/min with GHSV corresponding to 180000 mL·g⁻¹·h⁻¹. The reactant and product gases were measured using a quadrupole mass spectrometer in situ.

Acknowledgements

This work was supported by the Korea Institute of Energy Technology Evaluation and Planning (KETEP) and the Ministry of Trade, Industry & Energy (MOTIE) of the Republic of Korea (No. 20163030031850 and No. 20173010032120).

Conflict of Interest

The authors declare no conflict of interest.

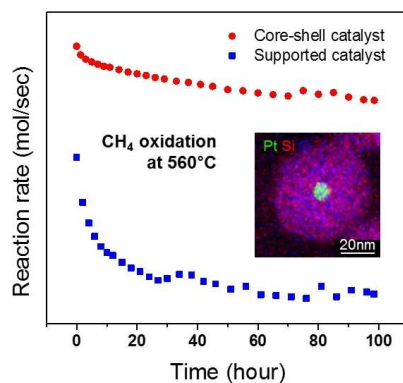
Keywords: Heterogeneous catalysis · Nanoparticles · Oxidation · Core-shell

- [1] a) K. Ding, A. Gulec, A. M. Johnson, N. M. Schweitzer, G. D. Stucky, L. D. Marks, P. C. Stair, *Science* **2015**, *350*, 189–192; b) J. Kim, Y.-S. Bae, H. Lee, *Nanoscale* **2014**, *6*, 12540–12546; c) C. Jiang, K. Hara, A. Fukuoaka, *Angew. Chem. Int. Ed.* **2013**, *52*, 6265–6268; *Angew. Chem.* **2013**, *125*, 6385–6388.
- [2] a) A. Cao, R. Lu, G. Vesper, *Phys. Chem. Chem. Phys.* **2010**, *12*, 13499–13510; b) T. W. Hansen, A. T. DeLaRiva, S. R. Challa, A. K. Datye, *Acc. Chem. Res.* **2013**, *46*, 1720–1730.
- [3] a) A. Cao, G. Vesper, *Nat. Mater.* **2009**, *9*, 75; b) X. Liu, A. Wang, X. Yang, T. Zhang, C.-Y. Mou, D.-S. Su, J. Li, *Chem. Mater.* **2009**, *21*, 410–418.
- [4] a) K. Zhao, B. Qiao, J. Wang, Y. Zhang, T. Zhang, *Chem. Commun.* **2011**, *47*, 1779–1781; b) H. Zhu, C. Liang, W. Yan, S. H. Overbury, S. Dai, *J. Phys. Chem. B* **2006**, *110*, 10842–10848.
- [5] a) S. Lee, J. Seo, W. Jung, *Nanoscale* **2016**, *8*, 10219–10228; b) M. Cargnello, J. J. D. Jaen, J. C. H. Garrido, K. Bakhmutsky, T. Montini, J. J. C. Gamez, R. J. Gorte, P. Fornasiero, *Science* **2012**, *337*, 713–717; c) Y. Choi, S. K. Cha, H. Ha, S. Lee, H. K. Seo, J. Y. Lee, H. Y. Kim, S. O. Kim, W. Jung, *Nat. Nanotechnol.* **2019**, *14*, 245–251; d) M. A. Lucchini, A. Testino, A. Kambolis, C. Proff, C. Ludwig, *Appl. Catal. B* **2016**, *182*, 94–101; e) K. Bakhmutsky, N. L. Wieder, M. Cargnello, B. Galloway, P. Fornasiero, R. J. Gorte, *ChemSusChem* **2012**, *5*, 140–148; f) B. Li, T. Gu, T. Ming, J. Wang, P. Wang, J. Wang, J. C. Yu, *ACS Nano* **2014**, *8*, 8152–8162.
- [6] a) K. Hori, H. Matsune, S. Takenaka, M. Kishida, *Sci. Technol. Adv. Mater.* **2006**, *7*, 678–684; b) Y. Hu, Y. Wang, Z.-H. Lu, X. Chen, L. Xiong, *Appl. Surf. Sci.* **2015**, *341*, 85–189; c) S. H. Joo, J. Y. Park, C.-K. Tsung, Y. Yamada, P. Yang, G. A. Somorjai, *Nat. Mater.* **2009**, *8*, 126–131; d) J.-G. Oh, H. Kim, *Curr. Appl. Phys.* **2013**, *13*, 130–136; e) N. Almana, S. P. Phivilay, P. Laveille, M. N. Hedhili, P. Fornasiero, K. Takanaabe, J.-M. Basset, *J. Catal.* **2016**, *340*, 368–375; f) K. J. Lin, L. J. Chen, M. R. Prasad, C. Y. Cheng, *Adv. Mater.* **2004**, *16*, 1845–+ +; g) C. Zhang, Y. M. Zhou, Y. W. Zhang, Z. W. Zhang, Y. M. Xu, Q. L. Wang, *Powder Technol.* **2015**, *284*, 387–395; h) K. An, Q. Zhang, S. Alayoglu, N. Musselwhite, J.-Y. Shin, G. A. Somorjai, *Nano Lett.* **2014**, *14*, 4907–4912; i) C. X. Zhang, S. R. Li, T. Wang, G. W. Wu, X. B. Ma, J. L. Gong, *Chem. Commun.* **2013**, *49*, 10647–10649.
- [7] a) J. Seo, S. Lee, B. Koo, W. Jung, *CrystEngComm* **2018**, *20*, 2010–2015; b) K. An, G. A. Somorjai, *ChemCatChem* **2012**, *4*, 1512–1524; c) M.-P. Pileni, *Nat. Mater.* **2003**, *2*, 145–150; d) X. Kou, S. Zhang, C.-K. Tsung, M. H. Yeung, Q. Shi, G. D. Stucky, L. Sun, J. Wang, C. Yan, *J. Phys. Chem. B* **2006**, *110*, 16377–16383.
- [8] a) S.-Y. Park, K. Han, D. B. O'Neill, G. Mul, *J. Energy Chem.* **2017**, *26*, 309–314; b) J. M. Krier, W. D. Michalak, X. J. Cai, L. Carl, K. Komvopoulos, G. A. Somorjai, *Nano Lett.* **2015**, *15*, 39–44; c) R. V. Maligal-Ganesh, K. Brashler, X. Luan, T. W. Goh, J. Gustafson, J. Wu, W. Huang, *Top. Catal.* **2018**, *61*, 940–948; d) J. Martins, N. Batail, S. Silva, S. Rafik-Clement, A. Karelavic, D. P. Debecker, A. Chaumonnot, D. Uzio, *Catal. Commun.* **2015**, *58*, 11–15.
- [9] Y. Hu, K. Tao, C. Wu, C. Zhou, H. Yin, S. Zhou, *J. Phys. Chem. C* **2013**, *117*, 8974–8982.
- [10] A. Degen, M. Kosec, *J. Eur. Ceram. Soc.* **2000**, *20*, 667–673.
- [11] L. Foppa, J. Dupont, C. W. Scheeren, *RSC Adv.* **2014**, *4*, 16583–16588.
- [12] S. Kaneko, M. Izuka, A. Takahashi, M. Ohshima, H. Kurokawa, H. Miura, *Appl. Catal. A* **2012**, *427*, 85–91.
- [13] H. Lee, S. E. Habas, S. Kweskin, D. Butcher, G. A. Somorjai, P. D. Yang, *Angew. Chem. Int. Ed.* **2006**, *45*, 7824–7828; *Angew. Chem.* **2006**, *118*, 7988–7992.

Manuscript received: May 22, 2019
 Revised manuscript received: July 12, 2019
 Accepted manuscript online: July 16, 2019
 Version of record online: ■■■, ■■■■

FULL PAPERS

Is it really stable? Pt@SiO₂ core-shell catalysts with a uniform-sized Pt core and a mesoporous silica shell were synthesized. The evolution of reactivity to methane oxidation at high temperatures (> 500 °C) was analysed quantitatively compared with conventional Pt/SiO₂ catalysts.



S. Kim, S. Lee, Prof. W. Jung*

1 – 8

Sintering Resistance of Pt@SiO₂
Core-Shell Catalyst

